ECOTOXICITY OF HALLOYSITE NANOTUBE–SUPPORTED PALLADIUM NANOPARTICLES IN *RAPHANUS SATIVUS* L.

Lorenza Bellani,†‡ Lucia Giorgetti,‡ Serena Riela,*§ Giuseppe Lazzara,‖ Anna Scialabba,*#
and Marina Massaro§

†Dipartimento di Scienze della Vita, Università degli Studi di Siena, Siena, Italy
‡Istituto di Biolo, gia e Biotecnologia Agraria "CNR", Pisa, Italy
§Dipartimento STEBICEF, Sez. Chimica, Università degli Studi di Palermo, Palermo, Italy
‖Dipartimento di Fisica e Chimica, Università degli Studi di Palermo, Palermo, Italy
#Dipartimento STEBICEF, Sez. Botanica ed Ecologia vegetale, Università degli Studi di Palermo, Palermo, Italy

Abstract: Halloysite nanotubes (HNTs) are natural nanomaterials that are biocompatible and available in large amounts at low prices. They are emerging nanomaterials with appealing properties for applications like support for metal nanoparticles (NPs). The potential environmental impacts of NPs can be understood in terms of phytotoxicity. Current research has been focusing on HNT applications in cell or animal models, while their use in plants is limited so their ecotoxicological impact is poorly documented. To date there are no studies on the phytotoxic effects of functionalized halloysites (functionalized-HNTs). To develop a quantitative risk assessment model for predicting the potential impact of HNT–supported palladium nanoparticles (HNT-PdNPs) on plant life, an investigation was undertaken to explore their effects on seed germination, seedling development, and mitotic division in root tip cells of 2 lots of *Raphanus sativus* L. with different vigor. The results showed that exposure to 1500 mg/L of HNTs, functionalized-HNTs, and HNT-PdNPs had no significant influence on germination, seedling development, xylem differentiation, or mitotic index in both lots. Cytogenetic analyses revealed that treatments with functionalized-HNT significantly increased the number of aberrations in low-vigor seeds. These results suggest that low-vigor seeds represent a model for a stress test that would be useful to monitor the effects of NPs. Moreover the present study offers scientific evidence for the use of halloysite for environmental purposes, supporting the biological safety of HNT-PdNPs. *Environ Toxicol Chem* 2016;35:2503–2510. © 2016 SETAC

Keywords: Palladium nanoparticles   Halloysite nanotubes   Seed germination   Cytological analysis   *Raphanus sativus* L

INTRODUCTION

Halloysite nanotubes (HNTs) have been the focus of great interest in materials science because of their advantageous features such as environmental friendliness, biocompatibility, high porosity, and large surface area, as well as low cost and tunable properties [1,2]. The HNTs $(Al_2Si_2O_5(OH)_4 \times 2H_2O)$ are hollow aluminosilicate, similar to commonly used platy clay kaolin [3]. Generally HNTs are $0.2\,\mu m$ to $1.5\,\mu m$ long, and the inner and outer diameters of tubes are in the ranges of 10 nm to 30 nm and 40 nm to 70 nm, respectively. The HNT internal surface consists of gibbsite octahedral array (Al−OH) groups, whereas the siloxane groups (Si−O−Si) are mainly on the external surface. Because of this peculiar chemical composition, HNTs are materials with the typical features of silica and alumina nanoparticles (NPs). The proximity of the alumina and silica layers, and the presence of 2 molecules of water in the interlayer, cause sheets to curve and roll up, forming multilayer NTs morphologically similar to multiwalled carbon nanotubes (MWCNTs) [4,5]. The different chemical composition at the inner and outer surfaces of these clay NTs allows for a few feasible modification methods by immobilization of functional groups, which can open up some interesting applications [6–8]. Recently HNTs and functionalized-HNTs have been emerging as nanomaterials with appealing abilities, such as support for

metal NPs [9–11]. In particular, some researchers have recently functionalized the halloysite external surface with ionic liquid moieties [12–14]. It is well known that ionic liquids are able to stabilize metal NPs by electrostatic interactions [15].

The increasing application of HNT-NPs in catalysis necessitates an improved understanding of their potential impact on the environment, because industrial uses could lead to emissions of NPs into the atmosphere, hydrosphere, or geosphere [16–19].

Several recent studies have reported the investigation of halloysite nanotoxicity in vitro employing human cell cultures and microbial cells. The toxicity and cellular uptake of HNTs have been investigated using human breast cancer cells, epithelial adenocarcinoma cells, and anaplastic thyroid cancer cells [20,21]. The HNTs have been found to be a safe and useful nanomaterial, applicable for fabrication of novel drug delivery systems or biomedical implants [22,23].

Moreover, the interaction of HNTs with the microscopic algae *Chlorella pyrenoidosa* was also investigated. Lvov et al. demonstrated that there was no penetration of the nanomaterials into the interior of the cell because of electrostatic interactions between the cell wall surface and HNTs [24]. It was also reported that HNTs were safe for the freshwater ciliate protist *Paramecium caudatum* [25] and for the nematode *Caenorhabditis elegans* [26]. Similarly HNTs exhibit no toxicity to *Escherichia coli* bacteria [27] as well as yeast cells [28].

With regard to the nanomaterials that are chemically and morphologically similar to HNT (SiO_2 and Al_2O_3 NPs or MWCNTs), it has been reported that application of SiO_2NPs significantly enhanced seed germination and growth of tomato

---

seedlings [29]. In contrast, it has been demonstrated that the bioaccumulation of SiO₂NPs in Bt-transgenic cotton represented a potential risk for food crops and human health [30]. Yang and Watts [31] analyzed the phytotoxicity of Al₂O₃NPs in 5 plant species by root elongation experiments. They observed a reduction in root elongation as a result of toxic action related to the surface features of the NPs. The MWCNTs had no significant influence on germination percentage and root growth of 6 different crop species, including *Raphanus sativus* L. [32]. However, studies of the combined effects of NPs and metals on agricultural crops [33,34] provided limited information on the effects of NTs on plant development and cell differentiation.

We investigated the effects of palladium NPs supported on halloysite nanotubes (HNT-PdNPs) on seed germination, seedling growth and xylem differentiation, mitotic index, and chromosome aberrations in root tip cells using 2 lots of *R. sativus* L. with high and low vigor, respectively, to develop a quantitative risk assessment model for predicting the potential impact of HNT-PdNPs on plant life. To the best of our knowledge, no studies exist on the toxicity of HNTs in higher plants. Therefore the same studies were performed on octylimidazolium ionic liquid functionalized-HNTs, and for comparison, the effects of pristine HNTs were also explored. *Raphanus sativus* L. was chosen as a model plant because of its fast growth and high germination rate, its commercial relevance, and its high global consumption. The results support the use of halloysite for environmental purposes, as well as the biological safety of the HNT-PdNPs catalyst.

MATERIALS AND METHODS

Halloysite was purchased from Sigma-Aldrich and used without further purification. This material has an average tube diameter of 50 nm and inner lumen diameter of 15 nm. The typical specific surface area of this halloysite is 65 m²/g, the pore volume approximately 1.25 mL/g, the refractive index 1.54, and the specific gravity 2.53 g/cm³. The HNT-PdNPs were synthesized as recently described [13].

An ESEM FEI Quanta 200 F microscope was used to study the morphology of the functionalized-HNTs. Before each experiment, the sample was coated with gold under argon by means of an Edwards Sputter Coater S150A to avoid charging under the electron beam. The measurements were carried out in high vacuum mode ($<6 \times 10^{-4}$ Pa) for simultaneous secondary electron; the energy of the beam was 25 kV, and the working distance was 10 mm.

Dynamic light scattering and ζ-potential measurements were performed by means of a Zetasizer Nano ZS90 particle analyzer (Malvern Instruments). The field-time autocorrelation function was described by a monoexponential decay function, which provides the decay rate (Γ) correlated to the apparent diffusion coefficient for the translation motion $D = \Gamma/q^2$, where $q = 4\pi n \lambda^{-1} \sin(\theta/2)$ is the scattering vector, n the water refractive index, and θ the scattering angle.

Plant material

To evaluate the effects of HNT-PdNPs on the seed vigor of *R sativus* L. var. *tondo rosso precocissimo 2* (Fratelli Ingegnoli), the germination tests (%) were performed on 2 lots of seeds with different vigor, stored at 5 °C: 1 lot of high vigor collected in 2013 with a mean germination time of 30 h, and a second lot with low vigor collected in 2009 with a mean germination time of 34.7 h.

Seed germination and growth conditions

Germination tests were performed according to the International Seed Testing Association [35]. One hundred radish seeds of similar size were randomly selected, washed, and placed on Whatman filter paper in 4 groups of 25 seeds. Each group was placed on a Petri dish in the presence of 10 mL of different HNTs. Concentrations of up to 1500 mg/L (100 mg/L, 500 mg/L, 1000 mg/L, and 1500 mg/L) were used for pristine-HNTs, functionalized-HNTs, and HNT-PdNPs. Seeds were incubated at 25 °C in the dark, under continuous agitation. Deionized water was used as control. The number of germinated seeds was calculated after 24 h, 48 h, and 72 h of imbibition. Positive germination was scored on emergence of the root ($\sim$2 mm). All experiments were performed in quadruplicate, and the samples were used for further analyses.

Seed vigor was expressed as mean germination time calculated according to Bellani et al. [36].

$$MGT = \frac{\sum nt}{N} \qquad (1)$$

where *MGT* is the mean germination time, t is the time from the beginning of the germination test expressed in hours, n is the number of seeds newly germinated at time t; and N is the total number of seeds of final germination.

High-vigor or low-vigor seeds were either nonimbibed (dry seeds) or imbibed for 3 h, 6 h, 9 h, 24 h, 48 h, or 72 h. Fresh weight increase percentage (FWI %) was calculated as:

$$FWI\% = \frac{FWt_n - FWt_0}{FWt_0} \times 100 \qquad (2)$$

where FWt_n is fresh weight at n hours, and FWt_0 is initial weight at 0 h.

Dry weight was established by placing the seedlings in an oven at 103 °C for 24 h to reach a constant weight.

Xylem differentiation

Roots of the same length were collected 72 h post sowing, fixed in formalin/acetic acid/alcohol (FAA), dehydrated in a graded series of ethanol solutions, and embedded in paraffin. Transverse and longitudinal 10-μm-thick sections were cut with a microtome (Reichert Jung 2050 Supercut motorized microtome) and stained with toluidine blue 0.05% in distilled water for transverse or methylene blue 1% in water for longitudinal sections. At least 10 semi-thin sections per treatment were observed under a light microscope (Zeiss Axioskop equipped with Axiocam MRc5).

Cytological analysis

For cytological analysis, primary roots collected 72 h after sowing were fixed in Carnoy's fixative (absolute ethanol:glacial acetic acid 3:1 v/v) for 24 h, hydrolyzed in HCl 1 N, squashed in 45% acetic acid, and stained with a Feulgen reaction [18]. Five roots were analyzed for each test scoring, with at least 1000 nuclei randomly selected from each slide. Thereafter, the percentage of dividing cells (mitotic index) and each either normal or abnormal mitotic stage was calculated.

Statistical analysis

All experiments were in triplicate, and data are expressed as mean ± standard error. The Statistica package (StatSoft) was

used for analyses. Analysis of variance (ANOVA) and a post hoc Tukey multiple range test were used to identify statistically significant differences between treatments. The significance level was set at $p < 0.05$.

RESULTS AND DISCUSSION

Characterization of nanomaterials

The HNT-PdNPs used in the present study were synthesized following a protocol reported elsewhere [13] (Figure 1). Briefly, 3-mercaptopropyl trimethoxysilane was grafted onto the external surface of HNT by microwave irradiation. Then positively charged octylimidazolium moieties were introduced by a thiol-ene reaction. The preparation of supported palladium NPs, whereby the metal catalyst can be linked by electrostatic interactions in the functionalized-HNT support, was achieved by anion exchange from Br^- to $PdCl_4^{2-}$ (an aqueous solution of Na_2PdCl_4 was used). The solid material, functionalized-HNT-$(PdCl_4^{2-})$, was recovered by filtration, and the Pd(II) was reduced to Pd^0 with $NaBH_4$ in ethanol. A weight percentage Pd of 0.7 was obtained for HNT-PdNPs, as determined by energy-dispersive X-ray measurement. The HNT-PdNPs were analyzed by scanning electron microscopy to assess their surface morphology. As shown in Figure 2, the tubular shape of the nanoclay was preserved on interaction with PdNPs.

Dynamic light scattering were carried out to evaluate particle size distribution in aqueous suspension. In particular, an average diffusion coefficient (*D*) of $(0.82 \pm 0.09) \times 10^{-12}\,m^2\,s^{-1}$ was obtained for HNT-Pd nanomaterials. This value is close to that for HNT $(0.94 \pm 0.05) \times 10^{-12}\,m^2\,s^{-1}$, indicating that the NTs possess the same diffusion dynamic behavior of single diffusive NTs and therefore no aggregation of the NPs occurred.

With the aim of showing possible changes in the NP–NP interactions, the ζ-potential in water was measured. The HNT-Pd nanomaterial had a negative ζ-potential value $(-15.3 \pm 0.8\,mV)$, close to that of HNT $(-19.5 \pm 1.5\,mV)$. Therefore the electrostatic NP–NP repulsions were not altered by the surface functionalization, because the charge was not significantly changed.

Effect of HNT-PdNPs on seed germination and growth endpoints

Seed germination and seedling growth are the initial steps of plant life cycle. To determine the effects of HNT-PdNPs on seed germination and growth, we analyzed the germination percentage and mean germination time of *R. sativus* seeds after treatment with different concentration of HNT-PdNPs. In addition, the effects on seed growth expressed as fresh and dry weights of the seedlings and as root length were studied.

High-vigor seeds were germinated in distilled water (control) and in aqueous medium supplemented with HNT-PdNPs (Table 1).

The results indicated that high-vigor seeds treated with HNT-PdNPs exhibited a germination percentage and mean germination time comparable to the control group at 48 h and
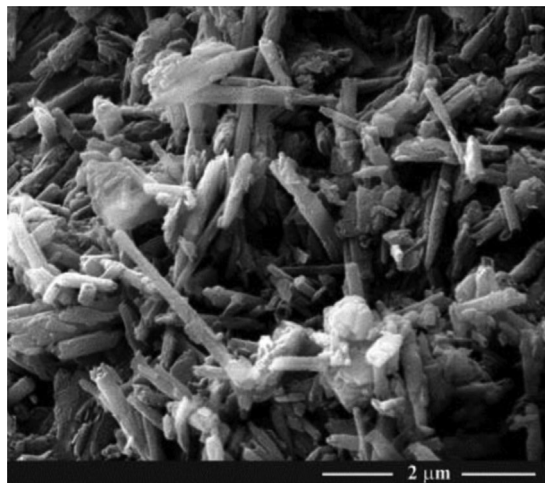

Figure 2. Scanning electron microscopy images of halloysite nanotube–supported palladium nanoparticles.

72 h of imbibition (Table 1), suggesting no environmental toxicity at the investigated concentrations. For comparison, we investigated the effects of pristine-HNT and functionalized-HNT on seed germination (Supplemental Data, Table S1).

These nanomaterials had no effect on germination percentage and mean germination time, consistent with their biocompatibility with living systems and their possible use in household materials and medicine [20].

Because seed vigor may directly influence the germination response, the effects of HNT-PdNPs were evaluated on low-vigor seeds with a final germination percentage similar to that of high-vigor seeds, but a slower germination speed. Low-vigor seeds were chosen because they represent a stress-sensitive biological system, allowing one to adequately predict the ability of seed survival under stress and adverse environmental conditions [37]. To rule out any possible effect on germination, the highest concentration of HNT-based nanomaterials was chosen (1500 mg/L).

As already observed for high-vigor seeds, these treatments did not significantly influence the germination percentage and mean germination time of low-vigor seeds compared to controls grown in water (Table 2).

Similar results were observed by Lin and Xing [32], who reported that NPs of aluminum, alumina, zinc, and zinc oxide did not affect radish germination. Other studies performed by Pj et al. [38] demonstrated that platinum NPs did not inhibit growth or germination of *R. sativus* seeds. Furthermore, $nCeO_2$ was shown to delay the germination of radish seeds but not to reduce germination percentage [39] or root growth [40]. Altogether, these studies suggest that the different nanomaterials exert distinctive effects on the germination response of the same species.

The effects of different HNT nanomaterials were further investigated on seedling growth, identified as fresh weight
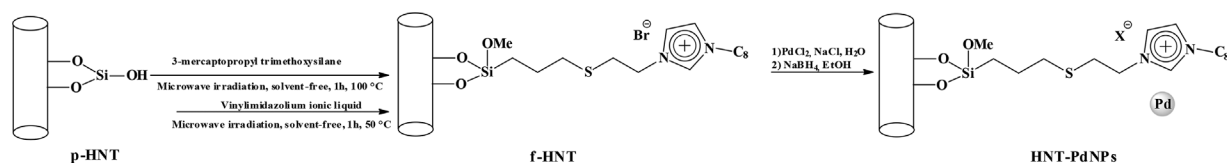

Figure 1. Representation of halloysite nanotube supported palladium nanoparticles synthesis. p-HNT = pristine halloysite nanotube; f-HNT = functionalized halloysite nanotube; HNT-PdNPs = halloysite nanotube supported palladium nanoparticles.

Table 1. Effects of several halloysite nanotube–supported palladium nanoparticle concentrations on germination percentage at different imbibition times and mean germination time at 72 h of radish seedlings from high-vigor seeds[a]

Treatment (HNT-PdNPs mg/L)	Germination %						MGT (h)	
	Incubation time (h)							
	24		48		72			
Control	73 ± 6	AB	95 ± 2	A	97 ± 2	A	30 ± 1	AB
100	84 ± 4	B	100	A	100	A	28 ± 1	A
500	60 ± 2	A	95 ± 3	A	96 ± 2	A	33 ± 1	B
1000	82 ± 2	A	96 ± 2	A	97 ± 2	A	28 ± 1	A
1500	83 ± 4	A	97 ± 2	A	98 ± 1	A	28 ± 2	A

[a]Values marked by different letters indicate significant differences according to Tukey's test within each incubation time.
HNT-PdNP = halloysite nanotube–supported palladium nanoparticle; MGT = mean germination percentage.

Table 2. Effect of 1500 mg/L of pristine halloysite nanotubes, functionalized halloysite nanotubes, and halloysite nanotube–supported palladium nanoparticles on germination percentage at different imbibition times and mean germination time at 72 h of radish seedlings from low-vigor seeds[a]

Treatment	Germination %						MGT (h)	
	Incubation time (h)							
	24		48		72			
Control	51 ± 4	A	90 ± 3	A	91 ± 3	A	34.7 ± 1.2	A
p-HNT	37 ± 5	A	91 ± 3	A	93 ± 3	A	38.9 ± 0.8	A
f-HNT	41 ± 7	A	94 ± 3	A	94 ± 3	A	37.5 ± 1.5	A
HNT-PdNPs	36 ± 4	A	88 ± 2	A	91 ± 3	A	39.2 ± 1.1	A

[a]Values marked by different letters indicate significant differences according to Tukey's test within each incubation time.
HNT-PdNP = halloysite nanotube–supported palladium nanoparticle; p-HNT = pristine halloysite nanotube; f-HNT = functionalized halloysite nanotubes; MGT = mean germination time.

increase, as dry weight, and as root elongation. Bewley [41] reported a triphasic pattern of water absorption for orthodox seeds: a rapid initial water uptake (phase I), followed by a plateau phase (phase II, lag phase), and a further increase (phase III), which occurs only after germination is completed, when the embryonic axes elongate. In the present study it was observed that in all treatments the first phase corresponded to a dramatic increase in fresh weight increase percentage in both high-vigor and low-vigor seeds up to 6 h of imbibition. The successive lag phase, which ends with the rupture of the seed coat and emission of the root, was prolonged from 9 h to 24 h in low-vigor seeds. The drastic increase in fresh weight increase percentage (phase III), observed for up to 72 h of imbibition, corresponded to seedling growth. At 48 h and 72 h of imbibition high-vigor seeds showed a fresh weight increase percentage that was double that of the corresponding low-quality seeds. This agrees with previous findings in *R. sativus* seeds [41] where artificial aging induced a reduction in fresh weight increase and a lengthening in the second phase. However, treatments with HNTs of seeds with high and low vigor had no significant influence on fresh weight increase percentage in respect to relative controls (Figure 3) whereas a significant increase in fresh weight increase percentage was observed at 48 h and 72 h of imbibition in pristine-HNT–treated high-vigor seeds. In addition, among the seedling growth parameters, dry weight was not significantly affected by HNT treatments in either high-quality or low-quality seeds (Supplemental Data, Table S2).
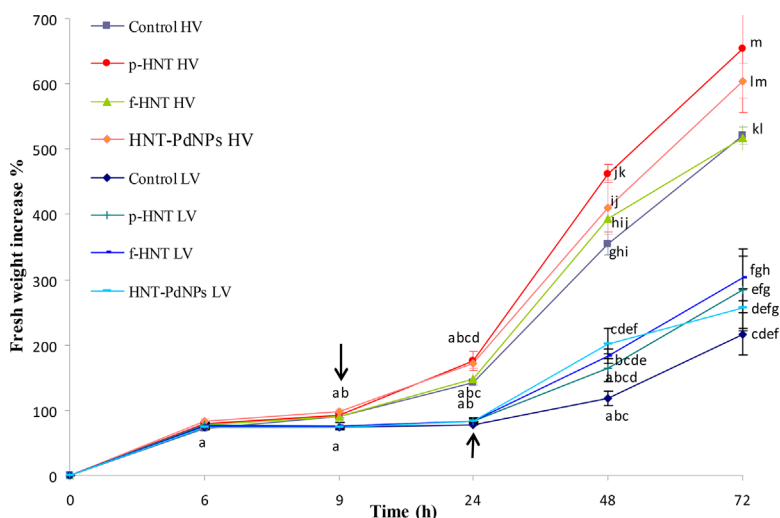

Figure 3. Effect of pristine halloysite nanotube (pristine-HNT), functionalized halloysite nanotube (f-HNT), and halloysite nanotube–supported palladium nanoparticle (HNT-PdNP) treatments on fresh weight increase percentage of radish seedlings from high and low vigor seeds. Arrows indicate visible radicle emergence. Values marked by different letters indicate significant differences according to Tukey's test between observations at different imbibition times and between control and treated high vigor and low vigor seeds. HV = high vigor; LV = low vigor.
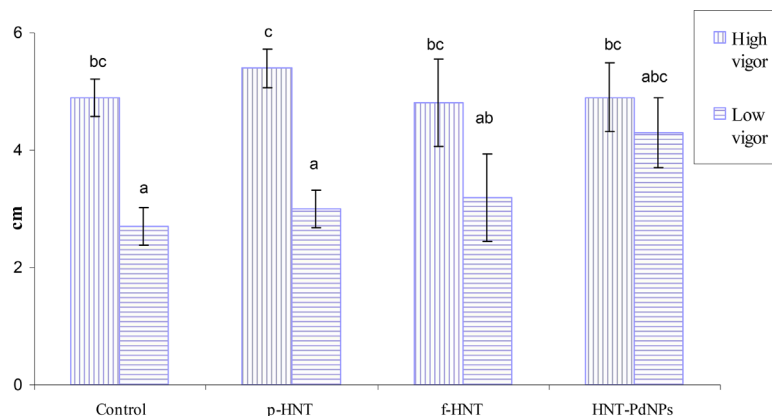
Figure 4. Effect of pristine halloysite nanotube, functionalized halloysite nanotube, and halloysite nanotube–supported palladium nanoparticle (HNT-PdNP) treatments on root length (expressed in cm) of radish seedlings from high-vigor and low-vigor seeds at 72-h imbibition. Values marked by different letters indicate significant differences according to Tukey's test between the 2 seed lots and between control and treated seeds. p-HNT = pristine halloysite nanotube; f-HNT = functionalized halloysite nanotube; HNT-PdNP = halloysite nanotube–supported palladium nanoparticle.

The effect of the NPs on radish root elongation was determined at 72 h (Figure 4). In both seed lots, no treatment had a significant impact on root elongation with respect to control, but seedlings from low-vigor seeds had shorter roots in both control and treated seedlings compared to seedlings from high-vigor seeds.

Our results for phytotoxicity of HNT to root elongation are different from the literature data that reported impairment of root growth for nonloaded alumina NPs in germinating seeds of

5 species (*Zea mays*, *Cucumis sativus*, *Glycine max*, *Brassica oleracea*, and *Daucus carota*) [31].

Effect of HNT-PdNPs on xylem differentiation and cytological modifications

In plants, the study of vascular tissue differentiation is essential to reach an understanding of seedling growth and development. For this reason, we wanted to rule out possible impacts of the nanomaterials analyzed on the differentiation of
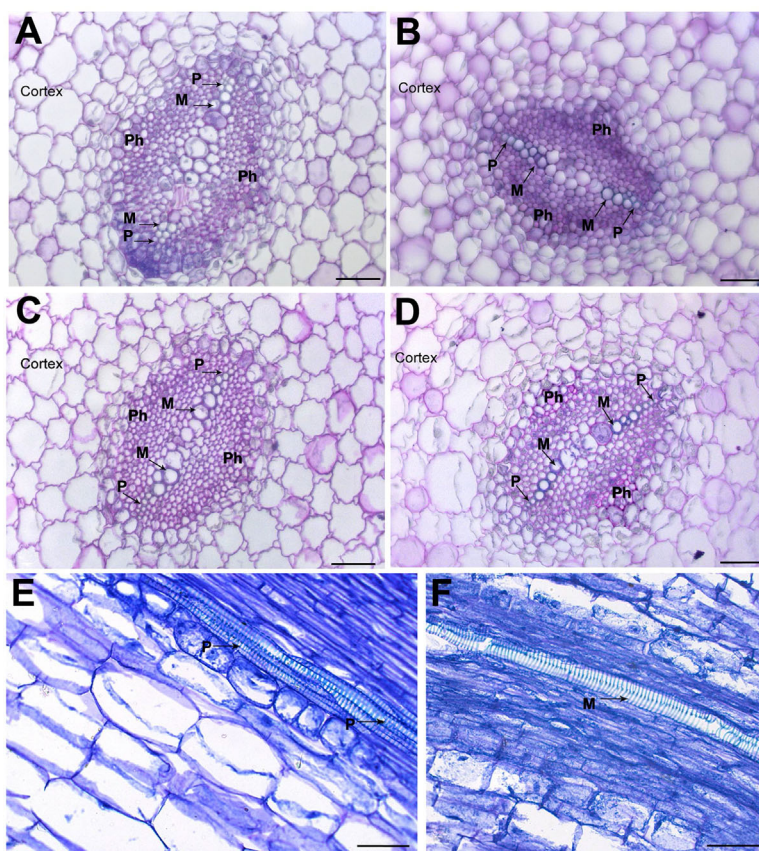

Figure 5. Effect of pristine halloysite nanotube (pristine-HNT), functionalized halloysite nanotube (functionalized-HNT), and halloysite nanotube–supported palladium nanoparticle (HNT-PdNP) treatments on root structure. Tranverse (**A–D**) and longitudinal (**E–F**) sections of radish roots from seedling at 72-h imbibition stained with toluidine blue (**A–D**) and methylene blue (**E,F**). Control (**A**); treated with: pristine-HNT (**B**), functionalized-HNT (**C**), and HNT-PdNPs (**D**). Control (**E**); functionalized-HNT (**F**). M = metaxylem; P = protoxylem; Ph = phloem. Scale bar = 50 μm.
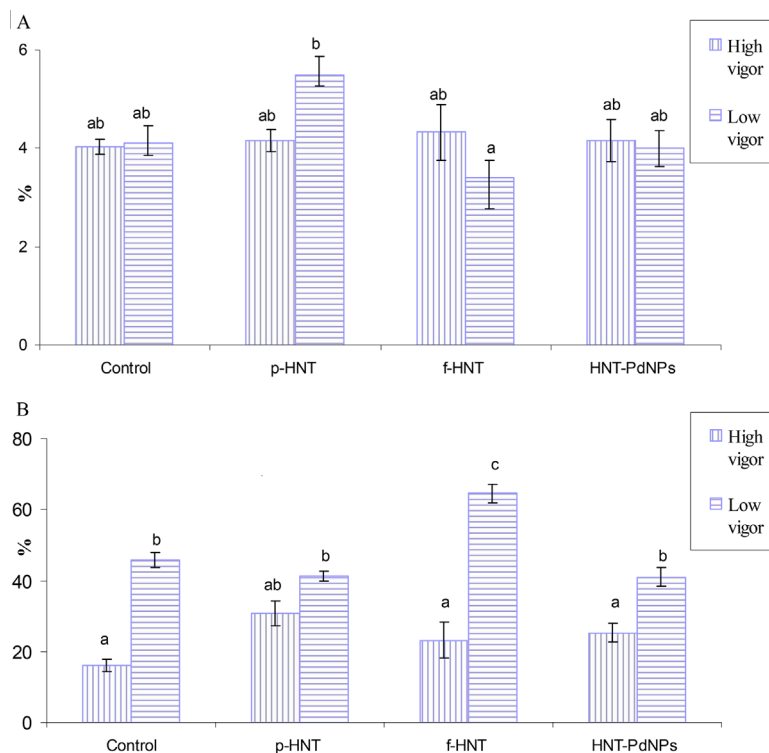
Figure 6. Effect of pristine halloysite nanotube, functionalized halloysite nanotube, and halloysite nanotube–supported palladium nanoparticle treatments on (**A**) mitotic index (%) and (**B**) chromosome aberrations (% of total divisions) of radish seedlings at 72-h imbibition from high-vigor and low-vigor seeds. Values marked by different letters indicate significant differences according to Tukey's test between the 2 seed lots and between control and treated seeds. p-HNT = pristine halloysite nanotube; f-HNT = functionalized-halloysite nanotube; HNT-PdNP = halloysite nanotube- supported palladium nanoparticle.

xylem elements, which are fundamental for water and mineral element transport and their distribution from the root to all plant organs.

A diarch structure, with phoem strands alternating with the xylem ridge, was observed on radish roots at 72 h of imbibition (Figure 5A–D, transversal sections, and E and F, longitudinal sections). In comparison with phloem elements, the xylem elements can be easily recognized by their secondary wall thickenings; therefore observations were performed on the latter tissue. At initial stages of vascular differentiation, the primary xylem consisted of a protoxylem in the outermost position with the narrowest xylem elements and helical or annular secondary wall thickenings visible in longitudinal sections (Figure 5E), and a metaxylem with later differentiation (Figure 5A–D) and wider elements showing secondary walls with helicoidal thickening (Figure 5F). Closer to the center, increasingly wider metaxylem elements were present. The xylem was not yet differentiated in the center of the root, showing immature metaxylem with no secondary cell wall lignification (Figure 5A–D). No differences were observed between control and treated seedlings in either low-vigor or high-vigor seeds (Figure 5A and E), thus evidencing that pristine-HNT (Figure 5B), functionalized-HNT (Figure 5C and F), and HNT-PdNPs (Figure 5D) had no effects on xylem differentiation.

Further cytogenetical analyses performed on radical meristems revealed no influence on the mitotic index of the tested treatments and no significant differences between high-quality and low-quality samples (Figure 6A). However, the analysis of chromosome aberrations, calculated as percentage of total mitotic divisions, provided additional invaluable information on seed quality because it reflected the damage induced by aging to the integrity of the genetic material. In fact, considering control low-vigor seeds, the percentage of chromosome aberrations in the seedling root meristem was significantly higher than in the corresponding seedlings from high-vigor seeds (45.7 % and 16.1 %, respectively; Figure 6B). Furthermore, treatments with functionalized-HNT significantly increased the number of aberrations in seedling root meristem from low-vigor seeds (Figure 6B).

Qualitative analysis of mitotic figures (Figure 7) revealed that in root meristem apices of seedlings from control high-vigor seeds, chromosomes appeared mostly normal (Figure 7A), whereas in seedlings from control low-vigor seeds many aberrations, mainly c-metaphases, were detected (Figure 7B). Treatments with HNT, functionalized-HNT, and HNT-PdNPs induced some alterations in chromosome morphology. In particular, c-metaphases (Figure 7C) and pyknotic nuclei (Figure 7D, E) with condensed chromatin and indistinguishable chromosomes (sticky chromosomes) were observed in pristine-HNT-treated samples. Cells with many cytoplasmic vesicles were observed in samples treated with functionalized-HNT (Figure 7F) and HNT-PdNPs. Lagging chromosomes at metaphase (Figure 7G) were observed in samples treated with functionalized-HNT. After treatment with HNT-PdNPs, chromosome bridges at anaphases (Figure 7H, I) and a few micronuclei (Figure 7J) were observed.

The anomalies detected in radish root meristems usually resulted from disturbances in the spindle apparatus (c-metaphases, anomalous anaphases, chromosome bridges), DNA strand breaks and chromosomal damage (lagging chromosome, fragments, micronuclei), as reported for *Vicia narbonensis* and *Zea mais* after treatment with nano-TiO$_2$ [18].
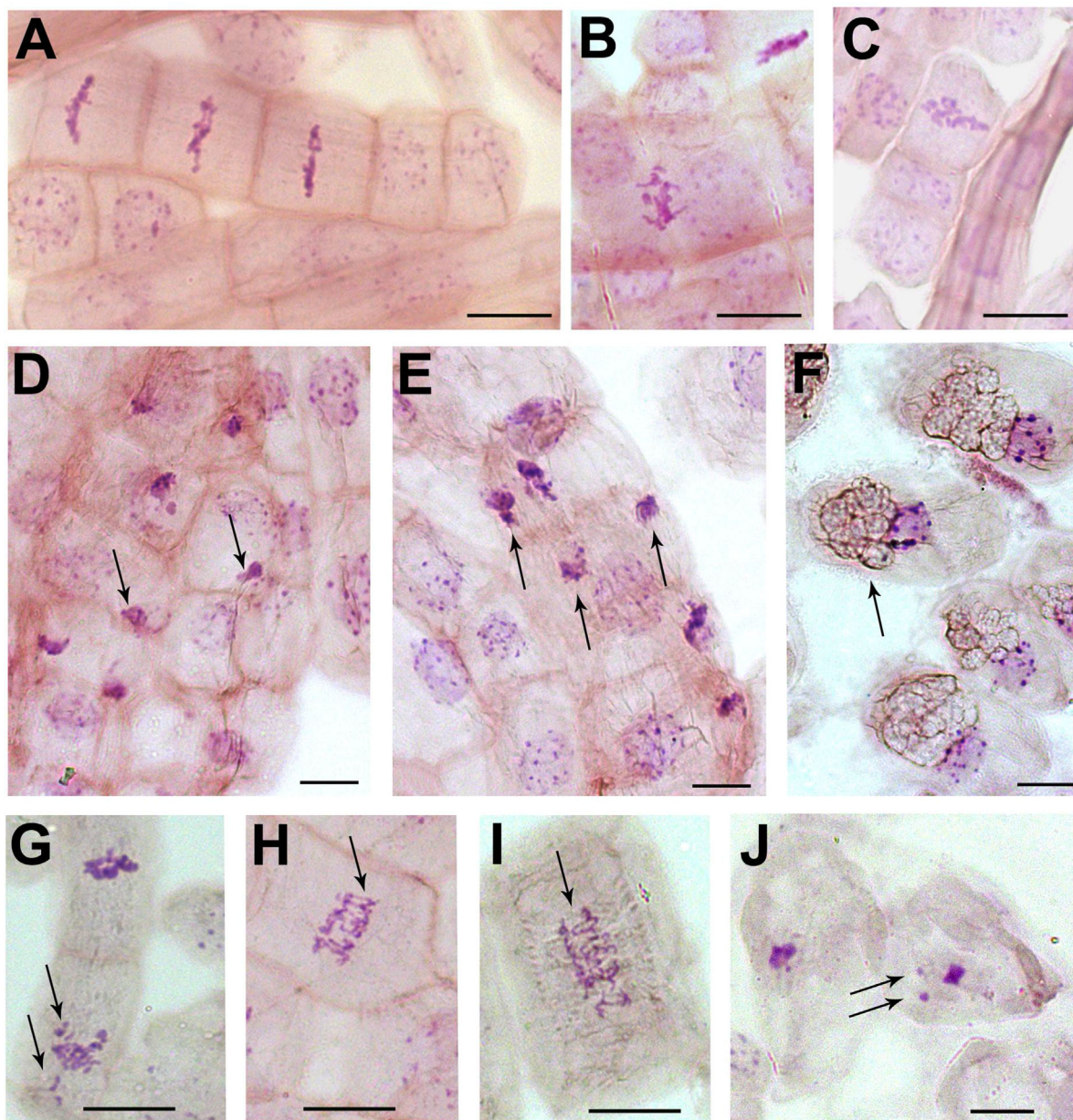
Figure 7. Effect of pristine halloysite nanotube (pristine-HNT), functionalized halloysite nanotube (functionalized-HNT), and halloysite nanotube–supported palladium nanoparticle (HNT-PdNP) treatments on mitotic figures of radish roots meristem 72-h imbibition from high-vigor and low-vigor seeds. High-vigor seeds treated with: water (**A**); pristine-HNT (**C**); functionalized-HNT (**F, G**); and HNT-PdNPs (**H**). Low-vigor seeds treated with: water (**B**); pristine-HNT (**D, E**); and HNT-PdNPs (**I, J**). Arrows indicate cytological anomalies, described in the text. Scale bar = 10 µm.

CONCLUSIONS

The present study has demonstrated that HNT-PdNPs (1500 mg/L) had no influence on radish seed germination physiology, seedling development and growth (expressed as fresh wt, dry wt, root length, and xylem differentiation), mitotic index, or chromosomal figures. Therefore the HNTs-PdNP nanomaterials are not phytotoxic to *R sativus* L. These results are in agreement with previous studies on the interaction of HNTs with living cells that possess cell walls similar to those of plants. Similarly, HNT-PdNPs cannot penetrate the cell interior because of the electrostatic interaction between the negatively charged cell surface and the positively charged HNT-PdNPs.

The analysis of chromosomal aberrations on root tips of low-vigor seeds revealed mild genotoxic effects, suggesting a sensitive and quantitative risk assessment model for analyses of the effects of novel NPs conjugates on plant life. In particular, the results obtained may serve as a useful reference for further research on the phytotoxicity of HNT-supported metal NPs.

REFERENCES

1. Liu M, Jia Z, Jia D, Zhou C. 2014. Recent advance in research on halloysite nanotubes-polymer nanocomposite. *Prog Polym Sci* 39:1498–1525.

2. Lvov Y, Abdullayev E. 2013. Functional polymer-clay nanotube composites with sustained release of chemical agents. *Prog Polym Sci* 38:1690–1719.

3. Massaro M, Riela S, Lo Meo P, Noto R, Cavallaro G, Milioto S, Lazzara G. 2014. Functionalized halloysite multivalent glycocluster as a new drug delivery system. *J Mater Chem B* 2:7732–7738.

4. Kamble R, Chag M, Gaikawad M, Panda BK. 2012. Halloysite nanotubes and applications: A review. *J Adv Sci Res* 3:25–29.

5. Lvov YM, Shchukin DG, Möhwald H, Price RR. 2008. Halloysite clay nanotubes for controlled release of protective agents. *ACS Nano* 2:814–820.

6. Abdullayev E, Abbasov V, Tursunbayeva A, Portnov V, Ibrahimov H, Mukhtarova G, Lvov Y. 2013. Self-healing coatings based on halloysite clay polymer composites for protection of copper alloys. *ACS Appl Mater Interf* 5:4464–4471.

7. Cavallaro G, Lazzara G, Milioto S, Parisi F, Sanzillo V. 2014. Modified halloysite nanotubes: Nanoarchitectures for enhancing the capture of oils from vapor and liquid phases. *ACS Appl Mater Interf* 6:606–612.

8. Massaro M, Colletti CG, Noto R, Riela S, Poma P, Guernelli S, Parisi F, Milioto S, Lazzara G. 2015. Pharmaceutical properties of supramolecular assembly of co-loaded cardanol/triazole-halloysite systems. *Int J Pharm* 478:476–485.

9. Zhang D, Huo W, Wang J, Li T, Cheng X, Li J, Zhang A. 2012. Synthesis of allyl-ended hyperbranched organic silicone resin by halloysite-supported platinum catalyst. *J Appl Polym Sci* 126:1580–1584.

10. Machado GS, de Freitas Castro KAD, Wypych F, Nakagaki S. 2008. Immobilization of metalloporphyrins into nanotubes of natural halloysite toward selective catalysts for oxidation reactions. *J Mol Catal A Chem* 283:99–107.

11. Barrientos-Ramírez S, Oca-Ramírez GMd, Ramos-Fernández EV, Sepúlveda-Escribano A, Pastor-Blas MM, González-Montiel A. 2011. Surface modification of natural halloysite clay nanotubes with aminosilanes. Application as catalyst supports in the atom transfer radical polymerization of methyl methacrylate. *Appl Catal A* 406:22–33.

12. Massaro M, Riela S, Cavallaro G, Colletti CG, Milioto S, Noto R, Parisi F, Lazzara G. 2015. Palladium supported on halloysite-triazolium salts as catalyst for ligand free Suzuki cross-coupling in water under microwave irradiation. *J Mol Catal A Chem* 408:12–19.

13. Massaro M, Riela S, Cavallaro G, Gruttadauria M, Milioto S, Noto R, Lazzara G. 2014. Eco-friendly functionalization of natural halloysite clay nanotube with ionic liquids by microwave irradiation for Suzuki coupling reaction. *J Organomet Chem* 749:410–415.

14. Massaro M, Riela S, Lazzara G, Gruttadauria M, Milioto S, Noto R. 2014. Green conditions for the Suzuki reaction using microwave irradiation and a new HNT-supported ionic liquid-like phase (HNT-SILLP) catalyst. *Appl Organomet Chem* 28:234–238.

15. Pârvulescu VI, Hardacre C. 2007. Catalysis in ionic liquids. *Chem Rev* 107:2615–2665.

16. Nair R, Varghese SH, Nair BG, Maekawa T, Yoshida Y, Kumar DS. 2010. Nanoparticulate material delivery to plants. *Plant Sci* 179:154–163.

17. Shaymurat T, Gu J, Xu C, Yang Z, Zhao Q, Liu Y, Liu Y. 2012. Phytotoxic and genotoxic effects of ZnO nanoparticles on garlic (*Allium sativum* L.): A morphological study. *Nanotoxicology* 6:241–248.

18. Ruffini Castiglione M, Giorgetti L, Geri C, Cremonini R. 2011. The effects of nano-TiO$_2$ on seed germination, development and mitosis of root tip cells of *Vicia narbonensis* L. and *Zea mays* L. *J Nanopart Res* 13:2443–2449.

19. Chichiriccò G, Poma A. 2015. Penetration and toxicity of nanomaterials in higher plants. *Nanomaterials* 5:851.

20. Vergaro V, Abdullayev E, Lvov YM, Zeitoun A, Cingolani R, Rinaldi R, Leporatti S. 2010. Cytocompatibility and uptake of halloysite clay nanotubes. *Biomacromolecules* 11:820–826.

21. Massaro M, Piana S, Colletti CG, Noto R, Riela S, Baiamonte C, Giordano C, Pizzolanti G, Cavallaro G, Milioto S, Lazzara G. 2015. Multicavity halloysite-amphiphilic cyclodextrin hybrids for co-delivery of natural drugs into thyroid cancer cells. *J Mater Chem B* 3:4074–4081.

22. Dzamukova MR, Naumenko EA, Lvov YM, Fakhrullin RF. 2015. Enzyme-activated intracellular drug delivery with tubule clay nano-formulation. *Sci Rep* 5:10560.

23. Wei W, Minullina R, Abdullayev E, Fakhrullin R, Mills D, Lvov Y. 2014. Enhanced efficiency of antiseptics with sustained release from clay nanotubes. *RSC Adv* 4:488–494.

24. Lvov Y, Aerov A, Fakhrullin R. 2014. Clay nanotube encapsulation for functional biocomposites. *Adv Colloid Interface Sci* 207:189–198.

25. Kryuchkova M, Danilushkina AA, Lvov YM, Fakhrullin RF. 2016. Evaluation of toxicity of nanoclays and graphene oxide in vivo: A *Paramecium caudatum* study. *Environ Sci Nano* 3:442–452.

26. Fakhrullina GI, Akhatova FS, Lvov YM, Fakhrullin RF. 2015. Toxicity of halloysite clay nanotubes in vivo: A *Caenorhabditis elegans* study. *Environ Sci Nano* 2:54–59.

27. Zhang Y, Chen Y, Zhang H, Zhang B, Liu J. 2013. Potent antibacterial activity of a novel silver nanoparticle-halloysite nanotube nano-composite powder. *J Inorg Biochem* 118:59–64.

28. Konnova SA, Sharipova IR, Demina TA, Osin YN, Yarullina DR, Ilinskaya ON, Lvov YM, Fakhrullin RF. 2013. Biomimetic cell-mediated three-dimensional assembly of halloysite nanotubes. *Chem Commun* 49:4208–4210.

29. Siddiqui MH, Al-Whaibi MH. 2014. Role of nano-SiO$_2$ in germination of tomato (*Lycopersicum esculentum* seeds Mill.). *Saudi J Biol Sci* 21:13–17.

30. Le V, Rui Y, Gui X, Li X, Liu S, Han Y. 2014. Uptake, transport, distribution and bio-effects of SiO$_2$ nanoparticles in Bt-transgenic cotton. *J Nanobiotech* 12:50.

31. Yang L, Watts DJ. 2005. Particle surface characteristics may play an important role in phytotoxicity of alumina nanoparticles. *Toxicol Lett* 158:122–132.

32. Lin D, Xing B. 2007. Phytotoxicity of nanoparticles: Inhibition of seed germination and root growth. *Environ Pollut* 150:243–250.

33. Wang C, Liu H, Chen J, Tian Y, Shi J, Li D, Guo C, Ma Q. 2014. Carboxylated multi-walled carbon nanotubes aggravated biochemical and subcellular damages in leaves of broad bean (*Vicia faba* L.) seedlings under combined stress of lead and cadmium. *J Hazard Mater* 274:404–412.

34. Ahmed F, Arshi N, Kumar S, Gill SS, Gill R, Tuteja N, Koo BH. 2013. Nanobiotechnology: Scope and potential for crop improvement. In Media SSB, ed, *Crop Improvement Under Adverse Conditions*. Springer, New York, NY, USA.

35. International Seed Testing Association. 1993. International rules for seed testing. *Seed Sci Technol Suppl* 21:25–41.

36. Bellani L, Salvini L, Dell'Aquila A, Scialabba A. 2012. Reactive oxygen species release, vitamin E, fatty acid and phytosterol contents of artificially aged radish (*Raphanus sativus* L.) seeds during germination. *Acta Physiol Plant* 34:1789–1799.

37. Scialabba A, Giorgetti L, Bellani LM. 2014. Stress integrated tests and cytological analyses reveal *Brassica villosa* subsp. *drepanensis* seed quality decrease upon long-term storage. *Plant Biosyst* 148:1–10.

38. Pj S, Mukerjee A, Chandrasekaran N. 2013. Comparative assessment of the phytotoxicity of silver and platinum nanoparticles. *Proceedings*, International Conference on Advanced Nanomaterials and Emerging Engineering Technologies (ICANMEET-2013), Chennai, India, July 24-26, 2013, pp 391–393.

39. Corral-Diaz B, Peralta-Videa JR, Alvarez-Parrilla E, Rodrigo-García J, Morales MI, Osuna-Avila P, Niu G, Hernandez-Viezcas JA, Gardea-Torresdey JL. 2014. Cerium oxide nanoparticles alter the antioxidant capacity but do not impact tuber ionome in *Raphanus sativus* (L). *Plant Physiol Biochem* 84:277–285.

40. Ma Y, Kuang L, He X, Bai W, Ding Y, Zhang Z, Zhao Y, Chai Z. 2010. Effects of rare earth oxide nanoparticles on root elongation of plants. *Chemosphere* 78:273–279.

41. Bewley JD, Black M. 1994. *Seeds*. Plenum, New York, NY, USA.